Reassembly of contractile actin cortex in cell blebs

Guillaume T. Charras,[1] Chi-Kuo Hu,[1,2] Margaret Coughlin,[1] and Timothy J. Mitchison[1]

[1]Department of Systems Biology and [2]Graduate Program in Biological and Biomedical Sciences, Harvard Medical School, Boston, MA 02115

Contractile actin cortex is involved in cell morphogenesis, movement, and cytokinesis, but its organization and assembly are poorly understood. During blebbing, the membrane detaches from the cortex and inflates. As expansion ceases, contractile cortex reassembles under the membrane and drives bleb retraction. This cycle enabled us to measure the temporal sequence of protein recruitment to the membrane during cortex reassembly and to explore dependency relationships. Expanding blebs were devoid of actin, but proteins of the erythrocytic submembranous cytoskeleton were present. When expansion ceased, ezrin was recruited to the membrane first, followed by actin, actin-bundling proteins, and, finally, contractile proteins. Complete assembly of the contractile cortex, which was organized into a cage-like mesh of filaments, took ~30 s. Cytochalasin D blocked recruitment of actin and α-actinin, but had no effect on membrane association of ankyrin B and ezrin. Ezrin played no role in actin nucleation, but was essential for tethering the membrane to the cortex. The Rho pathway was important for cortex assembly in blebs.

Introduction

The contractile cortex is a 50-nm–2-μm-thick layer of cytoskeleton under the plasma membrane that is rich in actin filaments, myosin II, and actin-binding proteins (Bray and White, 1988). Assembly dynamics and contractility of this layer are thought to generate cortical tension, drive cytokinesis, and play a central role in cell locomotion and tissue morphogenesis (Bray and White, 1988; Alberts et al., 2004). Despite its importance, the structural organization, dynamics, membrane connections, and assembly pathway of contractile cortex are not well understood. The classic unit of contractile actomyosin organization is the sarcomere, a structure that is well characterized in muscle cells and present in stress fibers of nonmuscle cells (Cramer et al., 1997; Alberts et al., 2004). However, typical contractile cortex does not contain well-organized sarcomeres by light or electron microscopy, and how its actin and myosin filaments are structurally organized is unclear.

Understanding the structure and dynamics of the cortex is important because it determines how cells respond to mechanical force or generate force for shape change and movement. Cells are composite materials, with each constituent conferring different mechanical properties. The membrane bilayer enables the maintenance of a specific microenvironment, but cannot expand or retain a stable shape when subjected to environmental forces (Hamill and Martinac, 2001). The plasma membrane of red blood cells is stiffened by a submembranous cytoskeleton consisting of a meshwork of spectrin tetramers tethered both to plasma membrane proteins and to short actin filaments by linking proteins, notably ankyrin and protein 4.1 (Bennett and Baines, 2001). Motile cells contain all of these proteins, but the extent and function of a submembranous cytoskeleton is unclear. They also have a much thicker and stiffer cortex under the plasma membrane, consisting of a shell of cross-linked actin filaments oriented tangential to the cell surface, which enables cells to better resist mechanical deformation (Bray and White, 1988). This shell can produce force either through myosin II–driven contraction or actin polymerization. Myosin-driven contraction generates cortical tension that can be converted into different types of motility by appropriate symmetry breaking (Bray and White, 1988).

Biochemically, the proteinaceous composition of the cortex is dominated by actin, actin-bundling proteins, and myosin II. How cortex is regulated and attached to the plasma membrane is unclear. The small GTPase RhoA is probably the most important regulator of contractile cortex assembly (Etienne-Manneville and Hall, 2002). Its activation leads to both actin polymerization and myosin II recruitment through several pathways in cytokinesis and chemotaxis (Lee et al., 2004; Bement et al., 2005; Kamijo et al., 2006), but its role in the regulation of generic contractile actin cortex is less well understood.

Correspondence to Guillaume Charras: gcharras@hms.harvard.edu

Abbreviations used in this paper: ERM, ezrin-radixin-moesin; FERM, four one ERM; GAP, GTPase-activating protein; GDI, guanine nucleotide dissociation inhibitor; GEF, guanine nucleotide exchange factor; MHC, myosin heavy chain; mRFP, monomeric red fluorescent protein; MRLC, myosin regulatory light chain; PH-PLCδ, PH domain of phospholipase C δ; PIP2, phosphotidylinositol bisphosphate; SEM, scanning electron microscopy; TEM, transmission electron microscopy; TDRFP, tandem dimer RFP.

The online version of this article contains supplemental material.

The Journal of Cell Biology, Vol. 175, No. 3, November 6, 2006 477–490
http://www.jcb.org/cgi/doi/10.1083/jcb.200602085

RhoA directly activates formins, which are actin-nucleating proteins that hold onto growing barbed ends (Higashida et al., 2004), and activates myosin II by regulation of its phosphorylation state through Rho-kinase (Totsukawa et al., 2000). The nature of the attachment of cortical actin to the membrane is poorly understood, despite identification of several protein candidates. In red blood cells, protein 4.1 links short actin filaments to integral membrane proteins, but its role in motile cells is less clear (Bennett and Baines, 2001). ERM (ezrin-radixin-moesin) proteins are natural candidates because they can bind both actin and integral membrane proteins (Bretscher et al., 2002). ERM proteins switch from an inactive closed conformation to an active open conformation that exposes an actin-binding site (at the tail) and a four one-ezrin-radixin-moesin (FERM) membrane–targeting domain (at the head; Bretscher et al., 2002). Perturbation experiments in cells are consistent with ERMs functioning in actin-membrane linkage (Gautreau et al., 2000).

One challenge in dissecting assembly of the contractile cortex in cells has been finding a starting point. The plasma membrane is almost always underlain by a cortex, and in situations like the assembly of the cytokinetic furrow, it is difficult to evaluate the relative contributions of de novo assembly at the furrow site versus sliding of cortical elements from neighboring membrane. One natural situation where cortex-free membrane is transiently generated is blebbing. This is a dramatic type of cell motility involving the contractile cortex that is often observed during apoptosis (Mills et al., 1998) and cytokinesis (Fishkind et al., 1991) and takes part in migration of some embryonic cells (Trinkaus, 1973). Bleb nucleation is initiated by the rapid detachment of a patch of membrane from the cortex. The patch is inflated over ~30 s to form a spherical protrusion that is 1–10 μm in diameter and filled with cytosol (Cunningham, 1995). When expansion stops, contractile cortex reassembles under the bleb membrane, and the bleb is retracted. Retraction finishes as the bleb cortex reintegrates the bulk cell cortex. Membrane detachment and bleb inflation are thought to be driven by intracellular pressure transients generated by myosin II contraction of the actin cortex. Indeed, drugs that relax the cortex by inhibiting actin or myosin II inhibit blebbing. We take advantage of blebbing as a window into the process of cortical assembly and dissect its assembly pathway.

Results

Bleb dynamics as a system to explore cortex assembly

Bleb expansion occurs when the membrane detaches from the actin cortical cytoskeleton. Imaging of constitutively blebbing

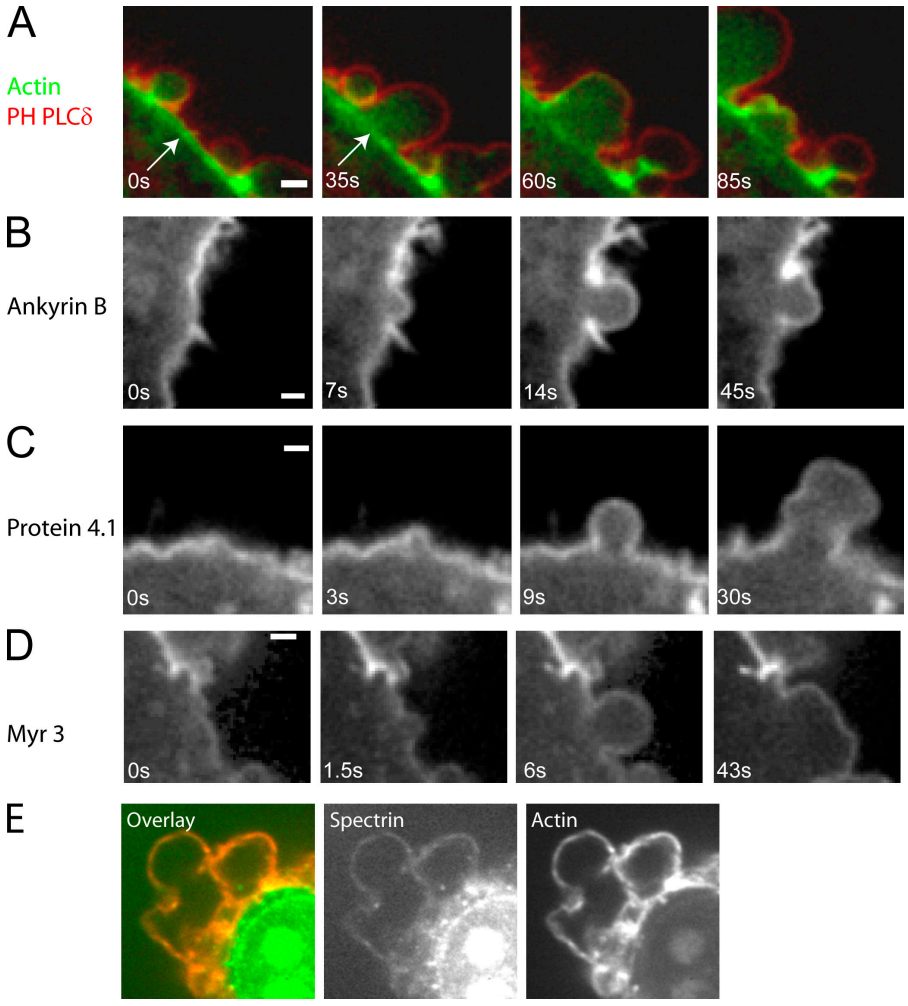

Figure 1. **Localization of proteins during bleb expansion and retraction.** All images were acquired using confocal microscopy. Timing relative to the first image is indicated in white text. (A) Localization of the membrane marker (the PH domain of PLCδ, red) and actin (green) during bleb expansion and retraction. The actin cortex is intact during bleb expansion (arrows) and is disassembled at later time points. (B–D) Ankyrin B (B), protein 4.1 (C), and myosin I (myr3, D) localize to the cell membrane throughout the life of a bleb. (E) Spectrin (green) colocalizes with actin (red) in retracting blebs. Bars, 1 μm.

M2 cells expressing both GFP-actin and a membrane marker, the PH domain of phospholipase C δ (PH-PLCδ), tagged with monomeric red fluorescent protein (mRFP) confirmed the absence of large amounts of actin in growing blebs and the persistence of an actin cortex in the cell body beneath the growing bleb (Fig. 1 A). Abundant cortical actin remains at the site of membrane detachment in the cell body during bleb expansion (Fig. 1 A, arrows). Actin is progressively recruited to the membrane during retraction (Fig. 1 A and Fig. 5, A–C). Thus, bleb dynamics provide a system to distinguish cortical proteins that associate constitutively with the plasma membrane from those that associate only when an actin cortex is present or assembling. We investigated the dynamics of 24 different cortical proteins in this system (Table I), selecting candidate proteins implicated in cortex–membrane attachment, actin organization, and contractility.

Proteins present during bleb expansion

Ankyrin B (Fig. 1 B) and protein 4.1 (nonerythroid isoform; Fig. 1 C), which are proteins of the erythrocyte cytoskeleton, formed a distinct rim of fluorescence at the bleb membrane, with no difference in intensity between expanding and contracting blebs. Myr 2 and 3, which are myosin I isoforms that target to the membrane (Barylko et al., 2000), exhibited similar dynamics (Fig. 1 D and not depicted). Thus, these proteins are constituents of a protein network that underlies the membrane at all times during bleb dynamics. We were unable to express full-length GFP-spectrin or GFP-adducin, but immunostaining revealed a distinct rim of spectrin (Fig. 1 E) and adducin (Fig. S1 B, available at http://www.jcb.org/cgi/content/full/jcb.200602085/DC1) at the bleb cortex in fixed cells. Because contracting blebs are better preserved than expanding blebs during fixation, these images most likely reveal association during or after actin assembly. We have no data on spectrin or adducin in expanding blebs, but suspect they must be present because proteins that associate with them (ankyrin B and protein 4.1) are present. In summary, a submembranous cytoskeleton is present at all times during the blebbing cycle, and the cytoskeleton of cortex-free expanding

Table I. **Protein composition of the principal cellular actin structures**

Protein	Technique	Bleb	Lamellipodium	Cytokinetic ring	Filopodia/microvilli	Phagocytotic cup
Ezrin	Immunostaining, GFP-tagging	Yes, between actin and membrane	Yes (Denker and Barber, 2002)		Yes (Bretscher, 1991)	Yes (Defacque et al., 2000)
Moesin	GFP-tagging	Yes				Yes (Defacque et al., 2000)
α-actinin	Immunostaining, GFP-tagging	Yes, colocalized with actin	Yes, mesh (Small et al., 2002)	Yes (Satterwhite and Pollard, 1992; Wu et al., 2003)	Yes (Bretscher, 1991)	Yes (May and Machesky, 2001)
Fimbrin	Immunostaining, GFP-tagging	Yes, colocalized with actin	Yes, mesh (Small et al., 2002)		Yes (Small et al., 2002)	
Fascin	GFP-tagging Immunostaining	No	Yes, mesh (Small et al., 2002)		Yes (Small et al., 2002)	
Filamin	Immunostaining	Yes (HeLa cells)	Yes, mesh (Stossel et al., 2001; Small et al., 2002)		Yes (Small et al., 2002)	Yes (May and Machesky, 2001; Stossel et al., 2001)
Anillin	Immunostaining, GFP-tagging	Yes		Yes (Straight et al., 2005; Wu et al., 2003)		
Coronin	GFP-tagging	Yes	Yes, mesh (Small et al., 2002)	Yes (Wu et al., 2003)		Yes (Rybakin and Clemen, 2005)
Septin	Immunostaining, GFP-tagging	No		Yes (Sanders and Field, 1994; Wu et al., 2003; Spiliotis et al., 2005)		
Tropomyosin	GFP-tagging, Immunostaining	Yes, colocalized with actin		Yes (Wu et al., 2003)	Yes (Bretscher, 1991)	
Tropomodulin	GFP-tagging	Yes				
Myosin II	Immunostaining, GFP-tagging	Yes, below the actin cortex	Yes, mesh	Yes (Satterwhite and Pollard, 1992; Wu et al., 2003)		
Myosin I	GFP-tagging	Yes			Yes (Bretscher, 1991)	
mDia1	GFP-tagging	No		Yes (Wu et al., 2003)		
Arp2/3	GFP-tagging, Immunostaining	No	Yes, leading edge and mesh (Small et al., 2002)			Yes (Castellano et al., 2001)
VASP	GFP-tagging, Immunostaining	No	Yes, leading edge (Small et al., 2002)		Yes (Small et al., 2002)	Yes (Castellano et al., 2001)
Adducin	Immunostaining	Yes				
Annexin II	GFP-tagging	No				
Capping protein	GFP-tagging	No	Yes (Small et al., 2002)	Yes (Wu et al., 2003)		

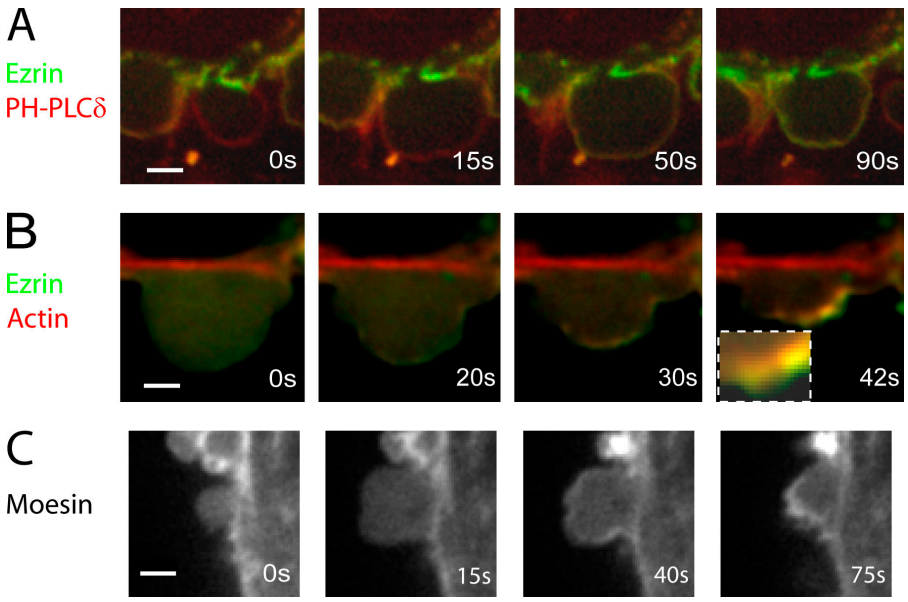

Figure 2. **Localization of ERM proteins during bleb expansion and retraction.** All images were acquired using confocal microscopy. Timing relative to the first image is indicated in white letters. (A) Ezrin (green) is initially absent from the membrane of expanding blebs. Once expansion stops, ezrin is recruited to the bleb and forms a continuous rim colocalized with the membrane. The bleb membrane (red) is visualized using the PH domain of PLCδ. (B) Ezrin (green) appears before actin (at 20 vs. 30 s) and forms a continuous rim external to the actin shell (red, inset). (C) Moesin is absent from the membrane of expanding blebs, but later forms a continuous rim. Bars, 2 μm.

blebs may resemble the rudimentary cytoskeleton that underlies the erythrocytic membrane.

ERM proteins are recruited early during bleb retraction

The transition from bleb expansion to stasis and, finally, contraction occurs over ∼30 s. This transition involves the recruitment of a new cortex to the membrane and provides a time window for measuring the relative timing of recruitment of cortical components, and testing dependency relationships. We imaged the recruitment dynamics of 18 different actin associated proteins. Eight did not localize to the bleb rim, and 10 transiently associated with the bleb rim (Table I and Figs. 2–4). We investigated the relative timing of the appearance of actin and six representative proteins that belonged to the three main classes of actin-binding proteins (linker proteins, bundling proteins, and proteins of the contractile apparatus) by measuring when the protein was first detectable above background at the

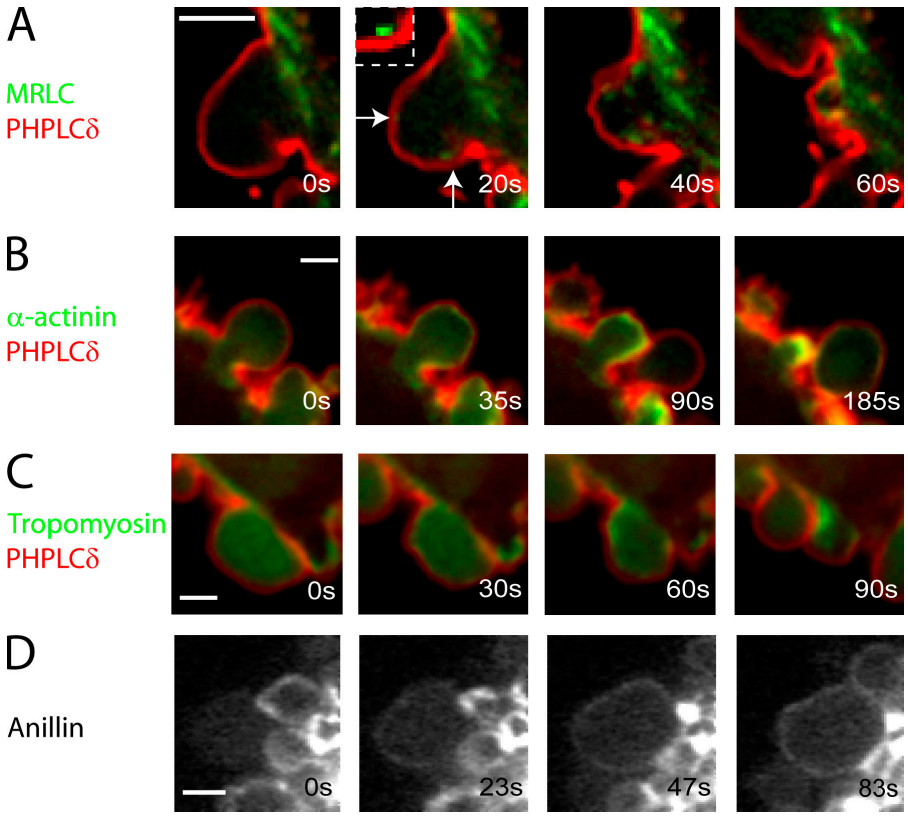

Figure 3. **Localization of proteins relative to the membrane during bleb retraction.** All images were acquired using confocal microscopy. The PH domain of PLCδ, a membrane marker, is visualized in red and the protein of interest in green. Timing relative to the first image is indicated in white text. MRLC (A) localizes to distinct foci (arrows and inset) under the bleb membrane in retracting blebs. α-Actinin (B), tropomyosin (C), and anillin (D) all form a continuous rim under the bleb membrane once expansion has stopped. Bars, 2 μm.

bleb rim, and then normalized this time to the time when actin recruitment was first detected at the rim (Fig. 5 D).

The first protein recruited was ezrin (Fig. 2, A and B), which links the actin cytoskeleton to the membrane. Ezrin was not enriched at the membrane during expansion, but rapidly localized to the bleb membrane as expansion slowed, forming a continuous rim colocalized with the membrane (Fig. 2 A). In two color videos, the actin rim was displaced toward the center of the bleb compared with the ezrin rim (Fig. 2 B, inset [t = 42 s], and Fig. S1 D), which is consistent with ezrin's role as a membrane linker (Bretscher et al., 2002). Recruitment of ezrin preceded recruitment of actin by 4.87 ± 3 s ($P_{actin} < 0.01$; $n = 23$; Fig. 2 B and Fig. 5 D). The delay between actin and ezrin recruitment could be visualized on two color kymographs (Fig. 5 A), where the newest cortex appears greener (ezrin rich/actin poor) compared with the older cortex (yellow). Moesin, another ERM family protein, had a localization similar to ezrin (Fig. 2 C).

Staged recruitment of other cortical proteins

Three actin-binding proteins were recruited shortly, but significantly, after actin itself. These were α-actinin (2.4 ± 4 s relative to actin, $n = 20$, $P_{actin} < 0.01$; Fig. 3 B, Fig. 5 B, and Fig. S1 A), coronin (1.5 ± 1.5 s relative to actin, $n = 23$, $P_{actin} < 0.01$; Fig. 4 B), and tropomyosin-4 (1.3 ± 1.5 s relative to actin, $n = 19$, $P_{actin} < 0.01$; Fig. 3 C and Fig. S1 H). All formed a uniform shell, exactly colocalized with actin, and presumably coassembled with new actin polymer. The timing of arrival of these proteins was not significantly different from one another (pairwise comparisons, $P > 0.29$). Fimbrin also assembled in a continuous rim colocalized with actin at the bleb periphery, but significantly later than the previous three (8.17 ± 4.9 s relative to actin, $n = 17$; Fig. 4 C and Fig. S1 E).

Myosin II recruitment to the bleb cortex is thought to drive bleb retraction. Myosin regulatory light chain (MRLC) was recruited significantly later than the early actin-binding proteins (7.3 ± 2.4 s relative to actin, $n = 27$, $P < 0.01$ for each pair-wise comparison with the early actin-binding proteins; Fig. 3 A, Fig. 4 A, and Fig. 5, C and D). Unlike other actin-binding proteins, MRLC and myosin heavy chain (MHC) assembled into small puncta that may represent contractile foci (Fig. 3 A, Fig. 4 A, Fig. S1 F, and not depicted).

Anillin (Fig. 3 D and Fig. S1 C) and tropomodulin (not depicted), proteins that regulate or interact with myosin II and actin (Fowler et al., 2003; Straight et al., 2005), were recruited to retracting blebs as a continuous rim, suggesting that they bind primarily to actin rather than myosin II.

Other proteins tested (i.e., VASP, Arp3, mDia1, fascin, capping protein, sept6, annexin II, tubulin, and vimentin) were not enriched in blebs by immunostaining or expression of full-length GFP-tagged constructs (unpublished data).

Cortical ultrastructure in retracting blebs

Three different electron microscopy techniques were used to probe bleb ultrastructure. Scanning electron microscopy (SEM) examination of blebbing cells fixed without permeabilization (Fig. 6 A) confirmed that fully extended blebs were approximately spherical and that retracting blebs displayed a crumpled morphology (Fig. 6 A, inset). Live observation

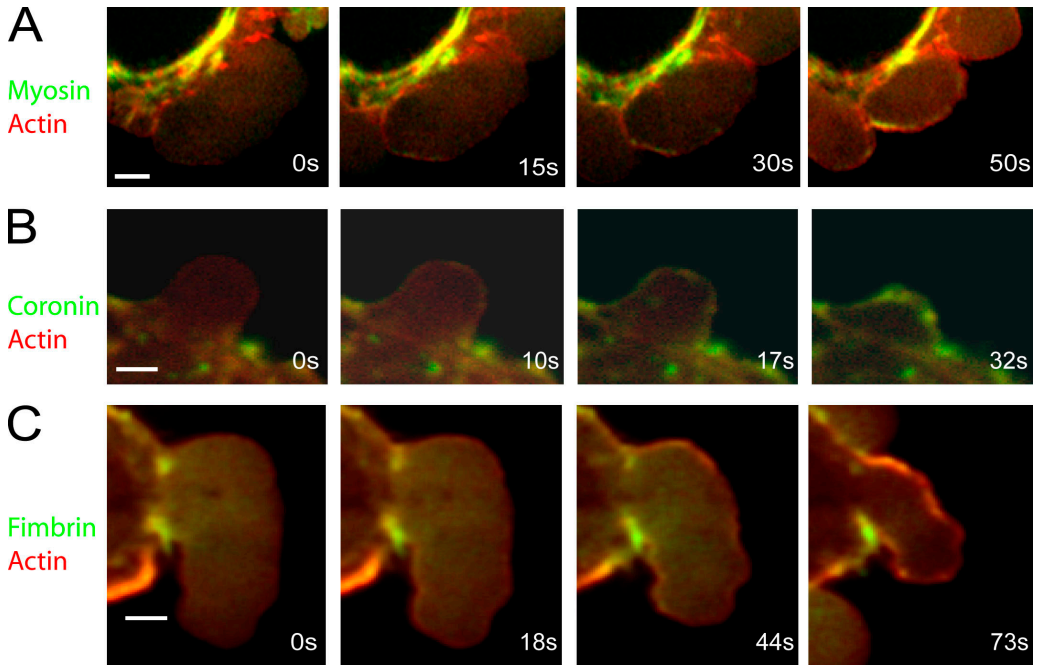

Figure 4. **Localization of proteins relative to actin during bleb retraction.** All images were acquired using confocal microscopy. In all images, actin is in red and the protein of interest in green. Timing relative to the first image is indicated in white text. (A) MRLC is originally not present (0–15 s) in the bleb, but assembles in distinct foci underneath the actin shell. (B) Coronin appears shortly after actin and forms a continuous rim colocalized with the actin shell. (C) Fimbrin appears after actin (44 vs. 18 s) and forms a continuous rim colocalized with the actin shell. Bars, 2 μm.

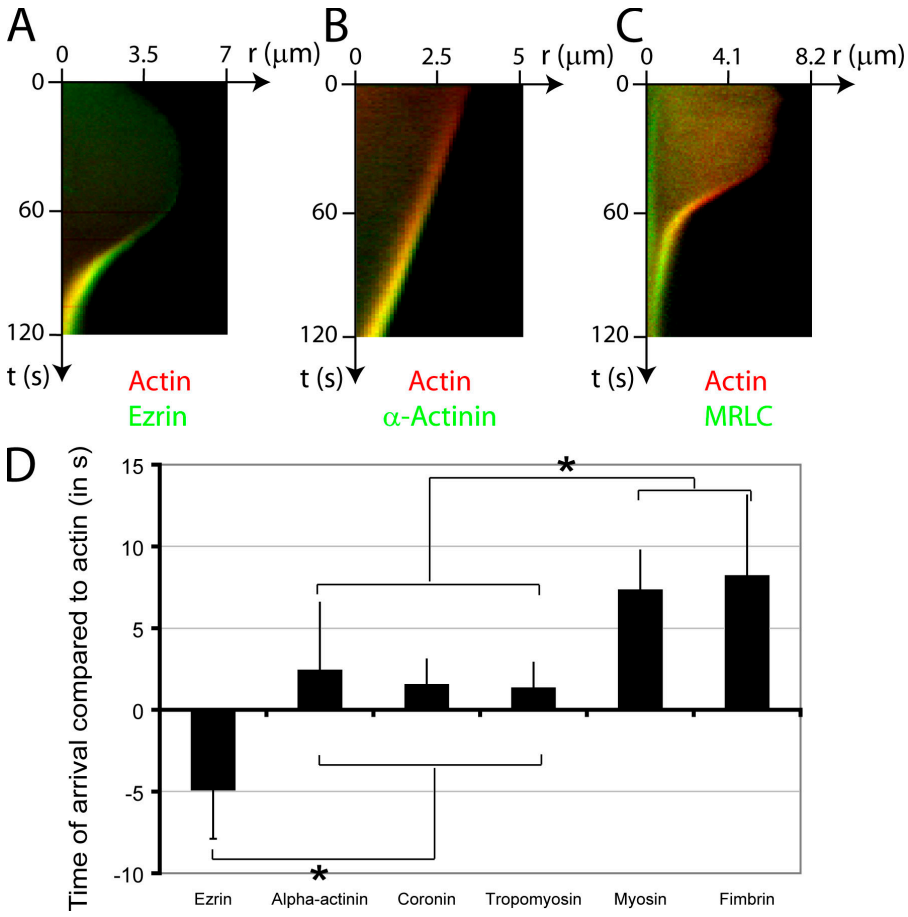

Figure 5. **Timing of arrival of actin binding proteins in the bleb relative to actin.** (A–C) Kymographs showing the localization of actin (red) compared with actin-binding proteins (green) during bleb retraction. Bleb extension is shown on the horizontal axis and time is shown on the vertical axis. Ezrin (A, green) arrives in the bleb significantly before actin and, consequently, a green trace can be seen at the bleb rim. As actin gets recruited to the rim, the trace turns yellow because of colocalization with ezrin. α-Actinin (B, green) and MRLC (C, green) are recruited after actin (red) and, consequently, a red trace can be seen first at the bleb rim. This trace turns yellow as these proteins are recruited to the rim. (D) Timing of arrival of the different actin-binding proteins in relationship to actin (t = 0 s). The error bars represent SD. Asterisks denote significant differences in timing. Ezrin arrives at the bleb rim significantly before actin. Coronin, α-actinin, and tropomyosin arrive significantly later than actin. Finally, fimbrin and myosin II appear last.

of cells during triton permeabilization, with or without simultaneous aldehyde fixation, showed that only retracting blebs survive permeabilization (unpublished data). Thin-section transmission electron microscopy (TEM) of saponin-permeabilized aldehyde-fixed cells revealed that the cortex of retracting blebs comprises a 10–20-nm-thick shell of actin filaments (verified by immunoTEM; not depicted) and shows clear signs of crumpling (Fig. 6 B). The best views of actin organization were provided by SEM examination of cells permeabilized in the presence of phalloidin to stabilize filamentous actin. Actin in retracting blebs formed an interconnected network resembling a cage (Fig. 6, C and D). Incubation of extracted cells with the S1 fragment of myosin revealed that all of the fibers within the cagelike structures were actin filaments (Fig. 6 D). Distinct knots were apparent at the vertices, but actin filaments' polarities showed no specific order around these (Fig. 6 D, arrow). Typical distances between adjacent vertices were 200 nm, or ~80 actin subunits, but this varied considerably between blebs, perhaps reflecting the age of the cortex, the degree of cross-linking, or how advanced contraction was. To test the generality of this organization, we examined blebs that occur naturally during cytokinesis in HeLa cells. Actin ultrastructure in HeLa blebs was identical, except that the actin mesh was tighter (Fig. 6 E). Interestingly, the cortex of HeLa cells arrested in metaphase had a similar morphology, but with a much tighter mesh (~20 nm; Fig. 6 F) and a thicker shell (50–100 nm; not depicted).

Actin dependence of protein recruitment

Timing alone can only suggest an assembly hierarchy, testing it requires perturbation experiments to reveal dependency relationships. The fast dynamics of the bleb cycle calls for fast perturbations, such as addition of cell-permeable drugs, but these are only available for a limited number of targets.

Treatment of blebbing cells with cytochalasin D, a drug that blocks actin polymerization at the barbed end, had two effects. At short times (~30 s), bleb initiation and expansion was stimulated; at longer times, blebbing was inhibited. This dual effect may arise because initially, the attachment between actin and the membrane is destabilized by cytochalasin D treatment, promoting bleb nucleation. At longer times, contraction of the cortex was compromised and new blebs ceased to appear. Blebs that had already formed an actin cortex before the onset of treatment were not affected and retracted normally (Fig. 7 A, white arrows). Conversely, blebs that emerged shortly after treatment did not assemble an actin rim and did not retract (Fig. 7 A, red arrows). This last effect allowed us to determine which proteins depend on actin for their recruitment to the bleb membrane.

To test the actin dependence of cortical protein recruitment, we imaged M2 cells transfected with GFP-tagged ankyrin B, ezrin, α-actinin, or coronin during cytochalasin D treatment. Cytochalasin D treatment did not affect either the localization or level of ankyrin B at the bleb membrane (Fig. 7 C). This was expected, given its constitutive targeting to the membrane.

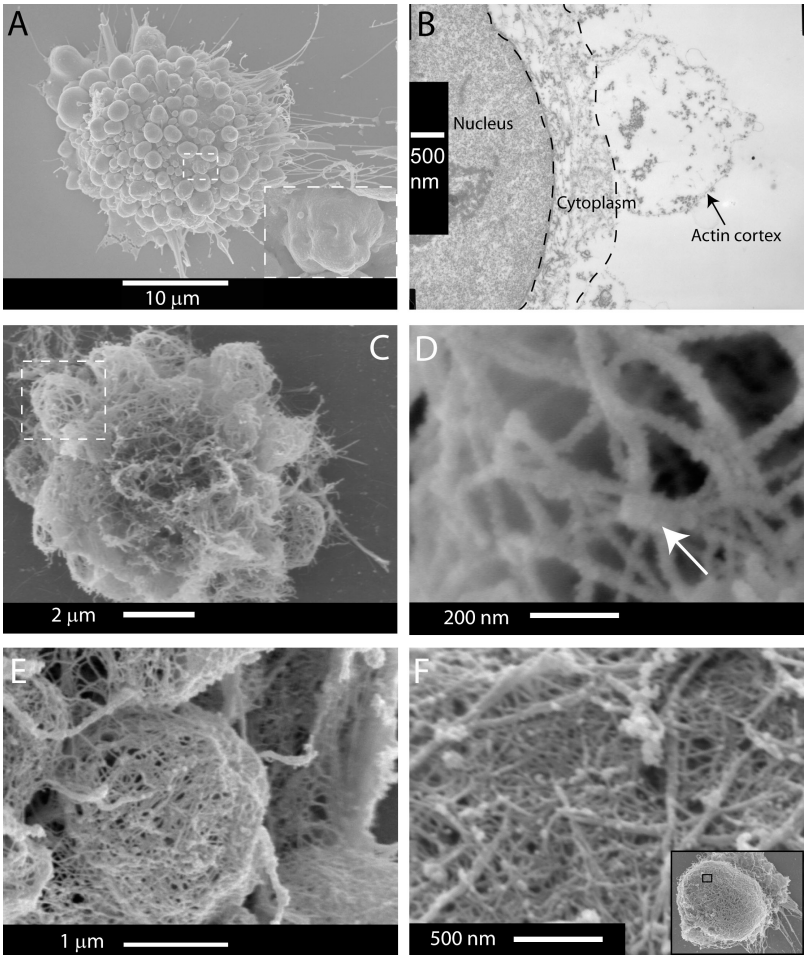

Figure 6. **Actin ultrastructure in retracting blebs.** (A) SEM of a blebbing cell with an intact cell membrane. (inset) As the retraction ends, the bleb membrane is crumpled. (B) TEM of the actin cortex of a retracting bleb. The bleb interior is devoid of cytoskeletal structures. Actin is concentrated at the bleb rim and forms a thin shell that is 10–20 nm thick. (C) Actin cytoskeleton of a blebbing cell. (D) Enlargement of boxed area in C. The cortex is formed by an entangled meshwork of actin with a few protuberant knots (arrow). The mesh size is ~200 nm. Myosin S1 head decoration shows no specific orientation of the actin around the knots. (E) Actin cytoskeleton of a bleb in a dividing HeLa cell. The morphology of blebs is similar to that of filamin-deficient cells, but the mesh is finer. (F) Actin cortex of a rounded HeLa cell. The morphology of the cortex is similar to that of blebs. The entire cell is shown in the inset.

α-Actinin was not recruited to the rim of blebs that emerged after the beginning of drug treatment and remained cytoplasmic (Fig. 7 B), which is consistent with coassembly of α-actinin and F-actin. Ezrin was still recruited to the membranes of blebs that formed after treatment (Fig. 7 E), and accumulated progressively at these membranes, giving a signal identical to that seen during the normal bleb cycle (cytochalasin, 76 ± 36%, $n = 20$ vs. control, 66 ± 31%, $n = 23$, $P = 0.34$). Thus, ezrin can target to membranes independent of actin and its localization, and kinetics are similar with and without actin. Coronin-3 was also recruited to blebs that formed after onset of treatment (unpublished data).

ERM proteins mediate cell–membrane attachment, but do not nucleate actin

The kinetics of ezrin recruitment, its response to cytochalasin D, and reports of ERM-mediated actin nucleation (Defacque et al., 2000), suggested an important role for this protein in cortex reassembly. To assess the role of ezrin in actin nucleation, we incubated cells expressing mRFP-actin and GFP-ezrin with drugs targeting reported regulators of ezrin (Lee et al., 2004). The only drug to have an effect on ezrin recruitment to the cell membrane was the broad-specificity kinase inhibitor staurosporine. Blebs that formed after staurosporine addition did not recruit ezrin to the bleb membrane, did form an actin rim, and did not retract (Fig. 7 D). Hence, ezrin localizes to the bleb rim earlier than actin but does not nucleate actin. Lack of retraction is presumably caused by inhibition of kinases that phosphorylate myosin. In blebs formed before staurosporine addition, ezrin fluorescence at the rim gradually decreased until it was no longer detectable above background. Drugs that targeted Rho-kinase (Y27632), protein kinase A (H89, K252C, and HA1077), protein kinase C (Go6976, K252C, and H9), tyrosine kinases (Genistein), G proteins (pertussis toxin and suramin), or phosphotidylinositol bisphosphate (PIP2; PBP-10; Cunningham et al., 2001) had no effect on ezrin localization to the bleb rim (unpublished data).

To further investigate the role of ezrin in bleb retraction, we perturbed ezrin function by overexpressing or microinjecting mutant forms of ezrin into cells expressing actin-GFP. Microinjection of recombinant FERM domain of ezrin-mRFP caused acute defects in bleb retraction. Actin was still recruited to the rim of blebs, but as retraction initiated the actin rim tended to tear away from the membrane, resulting in an inward flow of actin but complete or partial failure of membrane retraction (Fig. 8 A and Table II). Conversely, when recombinant ezrin-T567D-GFP was microinjected into blebbing cells, it localized to the submembranous cortex and inhibited blebbing, suggesting stabilization of actin–membrane links (Fig. 8 B and Table II). Stable expression of mutant forms of ezrin had effects consistent with

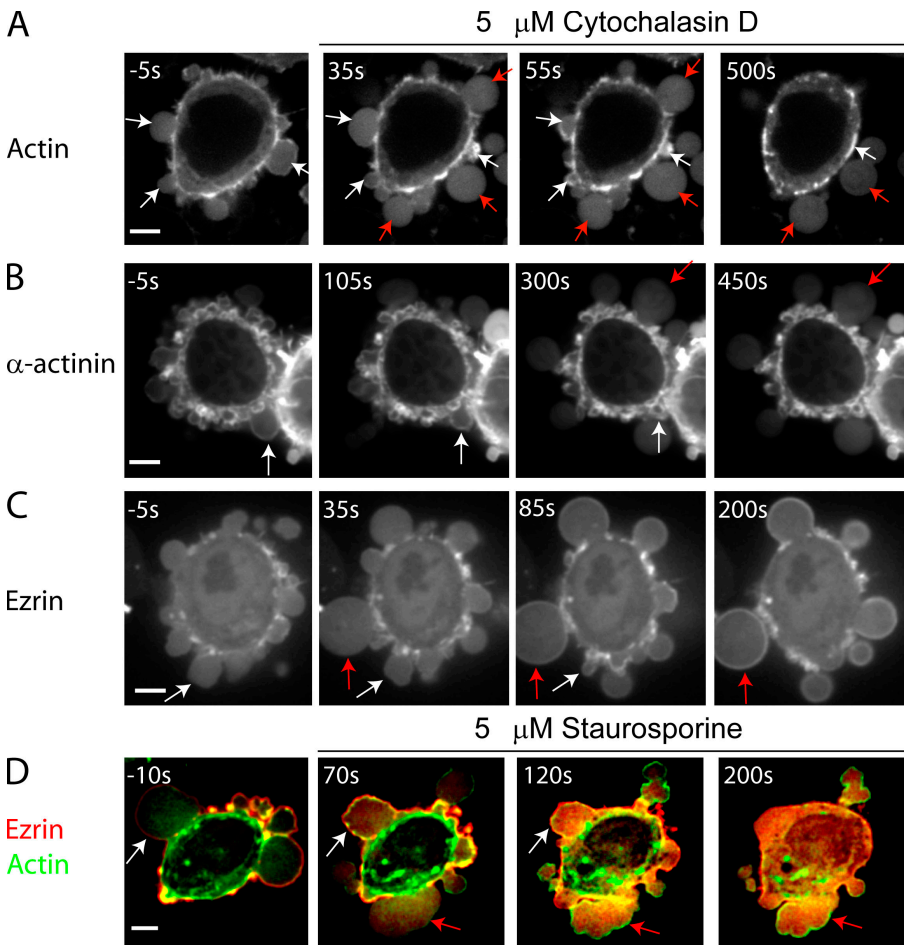

Figure 7. **Localization of actin and actin-binding proteins during bleb expansion and retraction in the presence of drugs.** Cytochalasin D, an actin depolymerizer, was added at time t = 0 s. All images were acquired using confocal microscopy. The timing of each image is indicated in white text. In all images, white arrows indicate blebs that have formed before the addition of cytochalasin D and red arrows indicate blebs that emerge after cytochalasin D treatment. (A and B) Actin (A) and α-actinin (B) localize to the rim of blebs that have formed before treatment and which continue to retract. Blebs that form after treatment do not retract and the proteins stay cytoplasmic. (C) Ezrin localizes to the rim of blebs that have formed before treatment, as well as to the rim of those formed after treatment. (D) In the absence of staurosporine, ezrin localizes to the bleb rim (white arrow, t = −10 s). Blebs that form after the addition of staurosporine (t = 0 s), do not recruit ezrin to their rim, but do still form an actin rim (red arrows). Treatment with staurosporine causes the relocalization of extant ezrin from the bleb rim to the cytoplasm (white arrows). Bars, 5 μm.

membrane–actin attachment, depending on ezrin function. M2 cells bleb profusely after plating, and the proportion of blebbing cells decreases over a period of days (Cunningham, 1995). Cells expressing dominant active ezrin-T567D-GFP stopped blebbing earlier than wild-type cells; whereas cells expressing either the FERM domain of ezrin-GFP or dominant-negative ezrin-T567A-GFP blebbed in higher proportion than wild-type cells (Fig. S2, available at http://www.jcb.org/cgi/content/full/jcb.200602085/DC1; Gautreau et al., 2000).

These data lead us to propose that ezrin serves to mechanically tether the plasma membrane to the forming actin cortex but does not participate in actin nucleation.

Myosin II powers bleb retraction

Studying the signaling events leading to bleb retraction is challenging because drugs that might inhibit retraction also inhibit general contractility of the actin cortex, making the effects on retraction alone difficult to interpret. To unambiguously examine

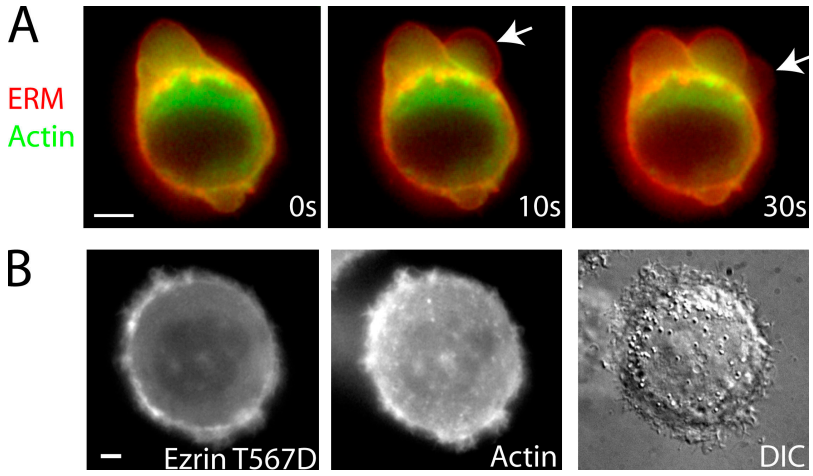

Figure 8. **Mutant forms of ezrin modulate the attachment of the cell membrane to the actin cytoskeleton.** All images were acquired using wide-field microscopy. Timing relative to the first image is indicated in white letters. (A) Microinjection of the FERM domain of ezrin tagged with mRFP into cells expressing actin-GFP fragilizes the attachment of the membrane to the actin cortex. In retracting blebs, the actin rim tended to tear away from the membrane (arrows at times t = 10 s and t = 30 s). This resulted in inwards flow of the actin rim, but the membrane failed to retract. (B) Microinjection of constitutively active ezrin (ezrin T567D) tagged with GFP into actin-mRFP–expressing cells causes the cessation of blebbing. Ezrin T567D colocalizes with actin at the cell periphery. Bars, 5 μm.

Table II. **Effect of microinjected reagents on proportion of blebbing cells**

Protein	Target protein	Concentration in the micropipette	Number of cells microinjected	Percentage of cells blebbing after microinjection	P value
Control (3kDa dextran)		100 μg/ml^{-1}	79	54	
Neomycin sulfate	PIP2	10 mM	14	57	0.8
FERM domain of ezrin	ERM proteins	600 μg/ml^{-1}	25	60	0.5
Ezrin T567D	ERM proteins	1.5 mg/ml^{-1}	21	5	<0.01
p50RhoGAP	Rho-GTPases	600 μg/ml^{-1}	15	33	<0.01
Rhotekin binding domain	RhoA	600 μg/ml^{-1}	40	35	<0.01
RhoGDIα	RhoA	1.2 mg/ml^{-1}	28	32	<0.01
C3-exoenzyme	Rho	100 μg/ml^{-1}	39	13	<0.01

regulation of retraction, we decoupled bleb retraction from expansion using a brief application (<2 min) of cytochalasin D, followed by washing out. This creates a population of stationary blebs devoid of actin that retract upon washout by recruiting actin and MRLC (Fig. 9 A). The steps leading to actin nucleation and retraction can be investigated by inclusion of inhibitors in the washout medium.

Inclusion of the myosin II ATPase inhibitor blebbistatin in the washout medium had no effect on actin rim formation, but inhibited retraction (Fig. 9 B). Upon inactivation of blebbistatin by exposure to blue light (Sakamoto et al., 2005), retraction resumed rapidly. In cells transfected with MRLC– tandem dimer RFP (TDRFP), blebbistatin did not inhibit recruitment of MRLC to the bleb rim (Fig. 9 C).

RhoA pathways regulate blebbing

The inhibitory effect of Rho-kinase inhibitors on blebbing suggested a role for the small GTPase RhoA. Immunostaining for active RhoA after TCA fixation (Kamijo et al., 2006; this preserves both expanding and retracting blebs; unpublished data) and expression of GFP-tagged RhoA revealed the presence of RhoA colocalized with the bleb membrane during all stages of blebbing (Fig. 10 A).

We investigated the effect of direct RhoA inhibition using proteins that affect RhoA activity. Microinjection of Rho guanine nucleotide dissociation inhibitor α (GDIα), the catalytic domain of p50Rho GTPase activating protein (GAP), the RhoGTPase-binding domain of rhotekin, or C3 exoenzyme lead to a significant decrease in the proportion of blebbing cells compared with controls (Table II). Unfortunately, in all cases, RhoA inhibition was too slow to assess its effect on actin nucleation or bleb retraction. Consistent with the microinjection results, overexpression of GFP-tagged RhoGDIα, rhotekin-binding domain, or p50RhoGAP lead to a significant decrease in the proportion of blebbing cells (Table III).

Localization of active RhoA at the cell membrane and the presence of ezrin within blebs directed our attention to Rho guanine nucleotide exchange factors (GEFs) reported to associate with ezrin, dbl and Net1 (Tran Quang et al., 2000; Vanni et al., 2004). GFP-tagged Net1 localized to the nucleus of blebbing cells (not depicted), but GFP-tagged KIAA0861, a GEF closely related to dbl (Rossman et al., 2005), colocalized

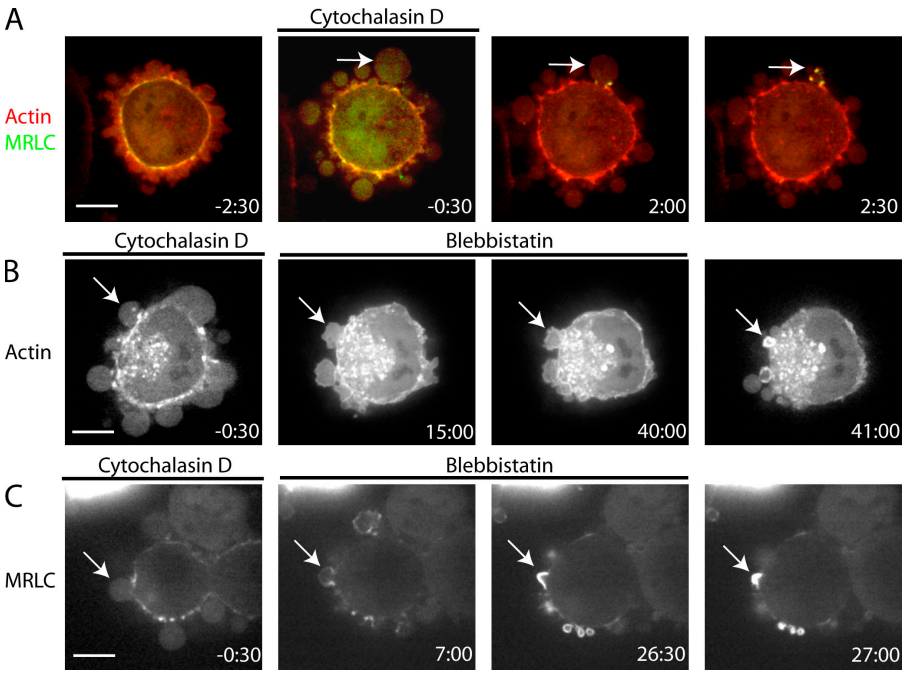

Figure 9. **Myosin II powers bleb retraction cytochalasin D, an actin depolymerizer, was added at time t = −2 min and treatment was pursued until t = 0 min.** Cytochalasin was washed out and, in some cases, blebbistatin was included in the washout medium. This second treatment was pursued for 15–50 min, and then a final washout or inactivation was effected. All images were acquired using confocal microscopy. The timing of each image in minutes is indicated in white text. (A) Blebs that emerged after the onset of treatment formed actin puncta (red), recruited MRLC (green) to puncta, and retracted upon washout (white arrow). (B) Inclusion of the myosin ATPase inhibitor blebbistatin in the washout medium did not prevent the formation of an actin rim but stopped retraction (white arrow). Upon blebbistatin inactivation (t = 50 min), retraction proceeded normally. (C) Inclusion of blebbistatin in the washout medium did not inhibit myosin recruitment to the bleb rim (white arrow). Upon blebbistatin inactivation (t = 27 min), retraction proceeded normally. Bars, 5 μm.

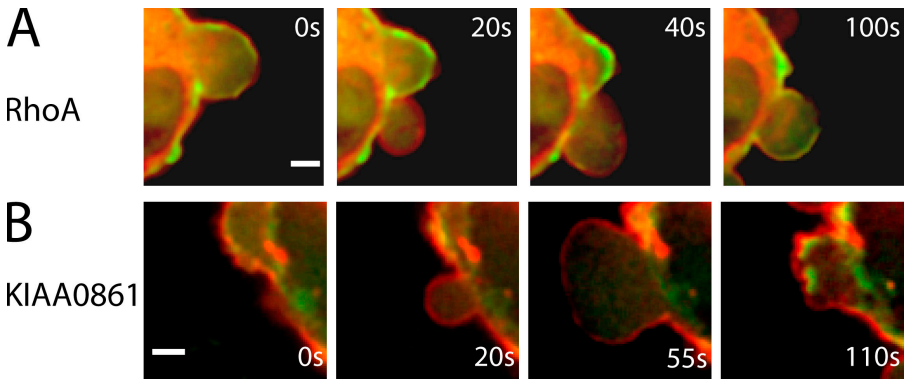

Figure 10. **Localization of RhoGTPase RhoA and the RhoGEF KIAA0861 during blebbing.** Timing relative to the first image is indicated in white text. All images were acquired using confocal microscopy. In all images, actin is shown in green and the protein of interest in red. Both RhoA (A) and the RhoGEF KIAA0861 (B) localized to the bleb membrane during all phases of blebbing. In both cases, the proteins were displaced toward the cell exterior when compared with actin. Bars, 2 μm.

with the cell membrane throughout all phases of blebbing (Fig. 10 B).

In summary, RhoA was present at the membrane during all phases of blebbing, microinjection, or overexpression of recombinant proteins that inactivated RhoA-inhibited blebbing, and KIAA0861, which is a RhoGEF closely related to dbl, was present at the membrane during all phases of blebbing. These data suggest that signaling downstream of RhoA is essential for blebbing; however, inhibition of Rho-GTPase activity was too slow to distinguish the role of RhoA in actin nucleation versus bleb retraction.

Discussion

Blebbing offers a window into the sequence of events leading to the reassembly of a contractile cortical actin cytoskeleton. One limitation of our study is that the accumulation of small quantities of proteins at the bleb cortex may be obscured by background fluorescence emanating from cytosolic protein. Indeed, we estimate that proteins must be ∼10% more concentrated at the cortex than in the cytosol for us to reliably image localization (unpublished data). We show that bleb retraction is the result of the sequential assembly of actin–membrane linker proteins, actin, actin-bundling proteins, regulatory proteins, and finally motor proteins.

Two proteins of the erythroid submembranous cytoskeleton, protein 4.1 and ankyrin B, were present at the membrane during all phases of blebbing, and both spectrin and adducin were present in retracting blebs. This suggested that an erythroid-like submembranous cytoskeleton may protect the cell membrane from lysis during the repeated cycles of bleb expansion and retraction. Nonerythroid cells have a spectrin-based network that extends over the entire cell surface; however, its function is unclear because microinjection of antibodies to spectrin that precipitated the network had no deleterious consequences in cells (Mangeat and Burridge, 1984). This may be because, under normal circumstances, the cell membrane is tethered to the actin cortex by ERM proteins independently from its attachment to the spectrin meshwork.

Ezrin played an important role in the stabilization of actin–membrane attachment in retracting blebs. Microinjection of the FERM domain of ezrin, which inhibits attachment of cellular ezrin to actin, weakened the actin–membrane attachment causing transient detachment of the actin cortex from the membrane during bleb retraction. Conversely, microinjection of a dominant active ezrin caused cessation of blebbing. These effects suggest that ezrin contributes strongly to actin–membrane adhesion energy. Decreasing the adhesion energy by impeding actin–membrane attachment increases bleb nucleation, whereas increasing the adhesion energy decreases bleb nucleation. Hence, two independent systems may coexist to protect the membrane from lysis. One, an erythroid-like submembranous cytoskeleton, is present during all phases of blebbing; the other tethers the membrane to the actin cytoskeleton via ERM proteins, is reassembled shortly after expansion ceases, and is regulated by an unknown staurosporine-sensitive kinase.

The actin cortex in newly formed blebs assembles into a cagelike structure cross-linked by actin-bundling proteins. The mechanism of actin nucleation beneath the membrane of newly formed bleb remains unclear, as neither Arp2/3 nor mDia1 localize to the bleb membrane. The role of RhoA in blebbing regulation suggests a role for a different formin in actin nucleation. The new actin cortex confers resistance to further expansion, as well as an essential framework for the transduction of forces generated by myosin-based movement. The cortical shell consisted of long criss-crossing strands of actin that intersected at ∼200-nm intervals, was 3–4 filaments thick, and was devoid of internal structures. Blebs from mitotic HeLa cells and the cortex of cells rounded in metaphase also had similar, but tighter, ultrastructures. Actin-bundling proteins rigidify actin gels by reducing their degrees of freedom. In blebs, actin-bundling proteins appeared later than actin, colocalized with the gel and presumably coassembled with it. Some actin-bundling proteins localized to the bleb rim shortly after actin (α-actinin and coronin), and significantly earlier than others (fimbrin). This may be caused by a difference in cross-linking distance (α-actinin,

Table III. **Effect of protein expression on proportion of blebbing cells**

Protein	Percentage cells blebbing	Number of cells	P value
GFP (Control)	58	98	
Rhotekin-binding domain	5	64	<0.01
RhoGDIα	5	70	<0.01
p50 RhoGap	0	37	<0.01

40 nm vs. fimbrin, 14 nm) that enables the longer ones to participate in early network assembly through a more efficient capture of surrounding actin filaments. As expected, the recruitment of α-actinin was dependent on the presence of an actin gel, but, surprisingly, the recruitment of coronin 3 was not, consistent with the hypothesis that it may play a role in reinforcing links between the actin cortex and the membrane (Spoerl et al., 2002). The final step was the assembly of the contractility control apparatus and the recruitment of motor proteins. Tropomyosin and tropomodulin, two proteins involved in the control of myosin contractility, are recruited to the bleb rim. Finally, myosin II localizes to discrete foci, which may correspond to minifilaments or ribbons of myosin (similar to the organization observed in lamellipodium; Verkhovsky et al., 1995) and these provide the force needed for retraction.

A central question in bleb dynamics is how cortex reassembly is triggered. We envisage two possibilities. First, cortex assembly is constitutive, but slow relative to bleb expansion. In this model, the expanding bleb is cortex free because of its rapid growth in area. When expansion slows, constitutive cortex assembly simply catches up. Cortex assembly may require a signaling pathway, but no special detection mechanisms to differentiate bleb membrane from generic membrane. The presence of both RhoA and a RhoGEF at the cell membrane at all stages of blebbing supports this model. In addition, ezrin may be recruited to the membrane via direct attachment to the RhoGEF (Vanni et al., 2004). In the second model, cortex assembly is triggered by an active signaling process downstream of some sensor that detects a change in the bleb membrane, such as membrane tension or exposed lipid head groups. In this model, cortex reassembly is locally triggered by a special property of the bleb membrane. For example, as the membrane tears from the actin cortex, PIP2 gets freed from its interaction partners, and this may provide an upstream signal for cortex reassembly. Another possibility is that the tension change concomitant with bleb expansion (Dai and Sheetz, 1999) could be detected by tension-sensitive mechanisms. Our data do not support either of these possibilities because treatment with chelators of PIP2 (neomycin sulfate and PBP10) or blockers of mechanosensitive channels (gadolinium chloride and GsMTx-4; unpublished data) had no effect on bleb retraction. Though, at present, our data seem to favor the constitutive assembly model, we cannot provide definitive evidence and more in-depth studies will be necessary.

Finally, Do our observations provide any clues as to the function of blebbing? Most animal cells bleb during cytokinesis and apoptosis, and some bleb during cell migration. Blebbing might simply be an epiphenomenon caused by strong activation of cortical contractility, or it might have a real function in these processes. Our observations reveal that blebbing efficiently triggers assembly of new cortex that can integrate into the bulk cortex as the bleb contracts. It might, thus, function as a pathway for new cortex generation when cells need to rapidly expand their cortical surface area, such as during cytokinesis. Consistent with this hypothesis, inhibition of actin polymerization at the poles of dividing cells inhibits cytokinesis more efficiently than inhibition at the furrow (Guha et al., 2005). As blebbing normally occurs at the poles during cytokinesis, it may be an efficient way of generating new cortex to increase cortical surface area while maintaining the furrow stable.

Materials and methods

Cell culture

Filamin-deficient M2 cells (Cunningham et al., 1992) were cultured in MEM with Earle's salts (Invitrogen) with penicillin/streptomycin, 10 mM Hepes, and 10% 80:20 mix of donor calf serum/fetal calf serum. All imaging was done in Leibovitz L-15 media (Invitrogen) supplemented with 10% 80:20 mix of donor calf serum/fetal calf serum. HeLa cells were cultured in DME (Invitrogen) with penicillin/streptomycin and 10% fetal calf serum.

Plasmid construction, mutagenesis, transfection, and recombinant protein purification

Detailed information about all of the plasmids used in this study is summarized in Table S1 (available at http://www.jcb.org/cgi/content/full/jcb.200602085/DC1). Unless otherwise noted, the full length of each gene was cloned.

Xenopus laevis MRLC and MHC tagged with GFP were gifts from A. Straight (Stanford University, Stanford, CA). Anillin-GFP was a gift from Field. mRFP and TDRFP were gifts from R. Tsien (University of California, San Diego, La Jolla, CA). The membrane was visualized by transfecting the cells with the PH domain of PLCδ tagged with GFP (a gift from T. Balla, National Institutes of Health, Bethesda, MD) or mRFP. Ankyrin B-GFP was a gift from V. Bennett (Duke University, Durham, NC). Moesin-GFP was a gift from H. Furthmayr (Stanford University). Myr2 and myr3-GFP were gifts from T. Lechler (Duke University). *X. laevis* tropomyosin 4-GFP, tropomodulin 3-GFP, and mDia1-GFP were gifts from N. Watanabe (University of Kyoto, Kyoto, Japan). Arp3-GFP and capping protein-GFP were gifts from D. Schafer (University of Virginia, Charlottesville, VA). Fascin-GFP was a gift from P. McCrea (University of Texas, Houston, TX). Sept6-GFP was a gift from M. Kinoshita (University of Kyoto). Vimentin-GFP was a kind gift from R. Goldman (Northwestern University, Chicago, IL). 6xHis-FERM domain of ezrin-mRFP was a gift from V. Gerke (University of Muenster, Muenster, Germany). Rhotekin-binding domain-GFP was a gift from W. Bement (University of Wisconsin, Madison, WI). 6xHis-Rhotekin binding domain-mRFP was a gift from R. Grosse (University of Heidelberg, Heidelberg, Germany). GST-tagged RhoA, RhoGDIGα, and p50RhoGAP were gifts from A. Hall (Memorial Sloan-Kettering Cancer Center, New York, NY). Actin-GFP and tubulin-GFP were purchased from CLONTECH Laboratories, Inc.

Ezrin (NM003379), coronin 3 (NM014325), annexin II (NM1002858), and fimbrin (NM005032) cDNA were obtained by RT-PCR from total mRNA extracts from M2 cells. Human Protein 4.1 (nonerythroid isoform, BC039079), human α-actinin (NM001102), human VASP (BC015289), human Net1 (BC053553), human KIAA0861 (BC064632), and human adducin (BC013393) cDNA were obtained from Opens Biosystems. The FERM domain of ezrin was obtained by RT-PCR of ezrin amino acids 0–309.

The full-length PCR products of ezrin, FERM domain, coronin, and protein 4.1 were directly ligated into pcDNA3.1-topo-GFP-CT (Invitrogen). Full-length α-actinin, adducin, annexin II, p50RhoGAP, RhoGDIα, RhoA, KIAA0861, Net1, and fimbrin PCR products were ligated into zero blunt vectors (Invitrogen), amplified, cut with the appropriate restriction enzymes, and ligated into GFP-C1, GFP-C3, or GFP-N1 (CLONTECH Laboratories, Inc.).

Actin localization was visualized by transfecting cells with an adenovirus containing GFP-tagged human β-actin (Charras et al., 2005). Alternatively, we used a melanoma cell line stably expressing actin-mRFP derived from wild-type M2 cells infected with actin-mRFP retrovirus in the retroviral vector pLNCX2 (CLONTECH Laboratories, Inc.).

For simultaneous examination of GFP-tagged actin and other proteins of interest (MRLC, MHC, tropomyosin, fimbrin, ezrin, PH-PLCδ, FERM, and α-actinin), we created mRFP variants of all of the aforementioned GFP-tagged protein constructs, except coronin, which was examined in conjunction with actin-mRFP.

Ezrin point mutations T567A (impaired actin binding and head-to-tail association) and T567D (constitutively active actin binding and impaired head-to-tail association; Gautreau et al., 2000) were performed using the one-step mutagenesis kit (Stratagene) on wild-type ezrin in pcDNA3.1-topo-GFP-CT. 6xHis-tagged ezrin T567D GFP was created by directly ligating the full-length PCR product of ezrin T567D GFP into pET100D (Invitrogen).

All gene products were verified by sequencing. Plasmid transfections were effected using Lipofectamine Plus (Invitrogen) according to the manufacturer's protocol, using 1 μg of cDNA per well of a 6-well plate (Invitrogen) and cells were examined the day after. In all cases tested, our GFP-tagged constructs of actin-binding proteins showed similar localization to immunofluorescence of endogenous protein (13 tested) or to localizations reported in the literature (9 proteins), and none of them perturbed blebbing significantly.

Recombinant protein expression and purification were effected using standard methods for His-tagged or GST-tagged protein purification. The purified proteins were either eluted directly or dialyzed overnight in either microinjection buffer (50 mM K-glutamate and 0.5 mM $MgCl_2$, pH 7.0) or in 50 mM KCl and 20 mM Tris-HCl, pH 7.0.

Western-blotting

For Western blotting, cells were scraped off the tissue culture dish in PBS, pelleted, resuspended in an equal volume of Laemmli buffer with β-mercaptoethanol, and boiled for 15 min. The samples were then loaded onto SDS-PAGE gels. Standard Western blotting techniques were used. Antibodies used (all monoclonal) were as follows: filamin A (1:1,000; CHEMICON International, Inc.), ezrin (1:2,000; Sigma-Aldrich), GFP (1:2,000; CLONTECH Laboratories, Inc.). HeLa cells were used as a positive control for filamin expression.

Immunostaining

For all antibodies except RhoA, the cells were fixed for 1 min at room temperature in a solution containing fixation buffer (137 mM NaCl, 5 mM KCl, 1.1 mM NaH_2PO_4, 0.4 mM KH_2PO_4, 2 mM $MgCl_2$, 2 mM K-EGTA, 5 mM Pipes, pH 6.8, and 5.5 mM Glucose) with 0.1% glutaraldehyde, 1% formaldehyde, and 0.3% Triton X-100. The cells were then fixed for 10 min further at room temperature in fixation buffer with 0.5% glutaraldehyde. For active RhoA staining, the cells were fixed with 10% TCA for 15 min on ice and treated as above. Monoclonal anti-RhoA antibody was purchased from Santa Cruz Biotechnologies, Inc. and used at 1:100 dilution. Cells were then stained using standard immunostaining techniques (Charras and Horton, 2002). Rhodamine-labeled phalloidin, monoclonal anti–α-actinin, polyclonal anti-vimentin, monoclonal anti-ezrin, monoclonal anti-MRLC, monoclonal anti-tropomyosin, and monoclonal anti-tubulin were purchased from Sigma-Aldrich and used at a 1:200, 1:200, 1:40, 1:100, 1:100, 1:100, and 1:500 dilutions, respectively. Polyclonal anti-spectrin, T-Plastin (fimbrin), and adducin antibodies were purchased from Santa Cruz Biotechnologies, Inc., and they were all used at 1:100 dilution. Polyclonal anti-myosin antibody was purchased from Biomedical Technologies and used at a 1:400 dilution. Monoclonal anti-anillin, polyclonal Arp3, and polyclonal VASP antibodies were gifts from C. Field (Harvard Medical School, Boston, MA), C. Egile (Harvard Medical School), and F. Southwick (University of Florida, Gainesville, FL), respectively, and they were used at 1:500, 1:500, and 1:100 dilutions. Monoclonal anti-fascin was from DakoCytomation and used at 1:100 dilution.

Confocal microscopy

All fluorescent imaging was done using a 1.3 NA 100× oil-immersion objective on an inverted microscope (Nikon TE-2000; Nikon) interfaced to a spinning disk confocal microscope (Perkin-Elmer) equipped with a heating stage heated to 37°C. Images were captured on a charge-coupled device camera (Orca ER; Hamamatsu) and acquired on a PC using Metamorph software (Molecular Devices). Images were acquired either 488-nm wavelength for GFP-tagged proteins and FITC-labeled secondary antibodies or with 568-nm wavelength for RFP-tagged proteins and TRITC-labeled secondary antibodies. For display, images were low pass filtered and scaled such that background fluorescence was minimal.

Measurement of appearance time for proteins

To assess the time of recruitment to the bleb rim of different proteins in relationship to actin, we cotransfected cells with actin-GFP or -mRFP and one of MRLC-TDRFP, α-actinin-mRFP, fimbrin-mRFP, tropomyosin-mRFP, coronin-GFP, or ezrin-mRFP. The next day, cells were imaged for 120 s at 1-s intervals. The intensity of both reporter constructs in retracting blebs was evaluated along a line drawn through the diameter using Metamorph (Molecular Devices). When one of the proteins appeared at the bleb rim, a clear peak in intensity above background could be observed. Actin was taken as the time reference and we measured the time of apparition of a fluorescence intensity peak at the bleb rim for each protein in comparison to actin. We collected peak appearance times for a maximum of 5 blebs per cell, for a minimum of 5 different cells for each protein, and a minimum of 17 blebs. For each protein, the time it appeared was compared with actin using a *t* test. Proteins were compared pairwise with a *t* test. Tests were considered significant if $P < 0.01$.

Drug treatments for assessment of dependence relationships

To assess whether F-actin was required for the recruitment of proteins involved in bleb retraction, we transfected cells with the protein of interest tagged with GFP and treated the cells with cytochalasin D (Sigma-Aldrich), a small molecule that promotes actin depolymerization by capping the fast-growing end of F-actin filaments. In all cases, the cells were first imaged for 20 time points at 5-s intervals to ascertain that the protein of interest localized normally. 5 μM cytochalasin D was added and the cells were imaged for an additional 100 time points.

To assess the dependence of actin recruitment on the presence of ezrin, we treated cells stably expressing actin-mRFP and transfected with ezrin-GFP with inhibitors to known regulators of ezrin, following a protocol identical to the one used with cytochalasin D. For ease of visualization, actin is shown in green in the figures and ezrin in red. The inhibitors used were Y27632 (25 μM; Calbiochem), H89 (20 μM; Calbiochem), K252C (50 μM; Calbiochem), HA1077 (20 μM; Sigma-Aldrich), Gö6976 (15 μM; Calbiochem), H9 (50 μM; Tocris), Genistein (100 μM; Calbiochem), pertussis toxin (1 $\mu g/ml^{-1}$), suramin (300 μM; Calbiochem), PBP-10 (10 μM; Calbiochem), and staurosporine (5 μM; Calbiochem).

To investigate the proteins and signaling events important for actin nucleation and bleb retraction, we transiently treated M2 cells transfected with actin-GFP and MRLC-TDRFP with 2.5 μM cytochalasin D for 2 min. This created a population of blebs devoid of actin that could reform an actin rim and recruit myosin once cytochalasin was removed. To remove cytochalasin, we exchanged medium 4 times. In experiments to determine how blebs retracted, we included blebbistatin (100 μM; Tocris) in the washout medium and treated for 10–50 min, then inactivated blebbistatin by exposure to 488-nm light for 600 ms (Sakamoto et al., 2005). During the whole procedure, images were acquired at 488 nm (except during blebbistatin treatment) and 568 nm every 10 s.

SEM of the cytoskeleton

For SEM imaging, cells were processed as described in Svitkina and Borisy (1998) with minor modifications. 2 h before treatment, cells were plated onto 12-mm glass coverslips. 10 min before, blebbing was stimulated by addition of fresh medium (Leibowitz L15 medium with 10% 80:20 DCS/FCS). The coverslips were washed 3 times with L15 without serum and transferred to extraction buffer for 20 min (50 mM imidazole, 50 mM KCl, 0.5 mM $MgCl_2$, 0.1 mM EDTA, 1 mM EGTA, 1% CHAPS, 2% Triton X-100, 2% PEG 35000, 10 μM phalloidin, and 1 $\mu l/ml^{-1}$ RNase cocktail (RNase T1 and A; Ambion), pH 6.8). For myosin S1 decoration of the actin filaments, the cells were incubated with 1 mg/ml^{-1} myosin S1 (Sigma-Aldrich) in cytoskeleton buffer (50 mM Imidazole, 50 mM KCl, 0.5 mM $MgCl_2$, 0.1 mM EDTA, and 1 mM EGTA, pH 6.8) for 30 min. The remainder of the protocol was identical to Svitkina and Borisy (1998). The cells were then dehydrated by exposure to serial ethanol dilutions, dried in an autosamdri-815 (Tousimis) critical point dryer, coated with 5–6 nm platinum-palladium and imaged using the in-lens detector of a SEM (Leo 892; Carl Zeiss MicroImaging, Inc.). For surface examination, cells were fixed for 10 min in 3% glutaraldehyde in cacodylate buffer, followed by a post-fix in tannic acid and uranyl-acetate. The sample was then prepared as above.

Thin sectioning TEM

For TEM examination, the cells were first permeabilized with 0.025% saponin in the same fixation buffer used for immunostaining for 1 min to release cytosol. They were fixed in fixation buffer with 1.5% glutaraldehyde and 50 mM lysine in 50 mM cacodylate, pH 7.0, for 6 min and post-fixed in 3% glutaraldehyde in cacodylate buffer for 6 min. For labeling experiments, the cells were then incubated with phalloidin-XX biotin (Invitrogen) for 30 min, followed by incubation with streptavidin–gold beads (EY laboratories). The remainder of the procedure was performed as described in Brieher et al. (2004).

Microinjection

Cells were plated onto glass coverslips the day before microinjection. Two cell populations were used for microinjection; wild-type M2 cells transfected with GFP-actin or M2 cells stably expressing actin-mRFP.

Microinjections were performed using standard procedures. In brief, borosilicate glass needles were pulled using a Sutter P-89. Before microinjection, the protein solution was centrifuged at top speed in a tabletop centrifuge to remove aggregates. Cells were microinjected with an Eppendorf 5242 microinjector (Eppendorf AG) using 30 hPa backpressure.

For proteins that were not fluorescently tagged, 100 μg/ml^{-1} 3-kD dextran-FITC (Invitrogen) was added to the protein solution. Recombinant C3-exoenzyme was a gift from K. Burridge (University of North Carolina, Chapel Hill, NC).

After microinjection, the cells were left to recuperate for at least 10 min. Cells that had been properly microinjected were identified by their fluorescence. Time-lapse videos of the cells were acquired over a period of 10 min–1 h after microinjection, using either a 40× objective for whole population studies or a 100× objective for localization studies. Time-lapse microscopy was performed on an inverted fluorescence microscope (TE300; Nikon) with a filter wheel. Images were acquired on a charge-coupled device camera and transferred to a PC computer using Metamorph software.

The proportion of blebbing cells within a microinjected population was evaluated by manually counting the total number of cells and the number of blebbing cells. The proportion of microinjected cells blebbing was compared with the proportion of cells blebbing after microinjection with 3-kD dextran-FITC, using a χ-square test with Yates correction.

Evaluation of the proportion of blebbing cells during transient protein expression

Cells were transiently transfected with GFP (control), p50RhoGAP-GFP, Rhotekin binding domain-GFP, or RhoGDIα-GFP. The proportion of blebbing cells within a transfected population was evaluated by manually counting the total number of transfected cells and the number of transfected blebbing cells. The effect of protein expression was evaluated by comparing the proportion of blebbing cells expressing the protein of interest to the proportion of blebbing cells expressing GFP only, using a χ-square test with Yates correction.

Online supplemental material

Fig. S1 shows protein localization in fixed blebbing cells using immunofluorescence. Fig. S2 shows that ezrin stabilizes cell shape. Fig. S3 shows localization of GFP-tagged ezrin mutants in spreading cells at different times after plating. Detailed information about all of the plasmids used in this study is summarized in Table S1. Online supplemental material is available at http://www.jcb.org/cgi/content/full/jcb.200602085/DC1.

The authors are grateful to Paul Chang for advice in establishing the stable cell lines. The authors wish to acknowledge fruitful discussions with Bill Brieher, Justin Yarrow, and Flann O'Brien. The authors wish to thank the Nikon Imaging Centre and its director, Dr J. Waters, at Harvard Medical School. The authors are thankful to the Center for Nanoscale Imaging at Harvard University and, in particular, to Drs. Schalek and Bell for their help.

G.T. Charras was supported by a Wellcome Trust Overseas Fellowship. T.J. Mitchison was supported by National Institutes of Health grant GM 48027.

Submitted: 14 February 2006
Accepted: 6 October 2006

References

Alberts, B., D. Bray, J. Lewis, M. Raff, K. Roberts, and J. Watson. 2004. Molecular Biology of the Cell. 4th edition. Taylor and Francis, New York. 1463 pp.

Barylko, B., D.D. Binns, and J.P. Albanesi. 2000. Regulation of the enzymatic and motor activities of myosin I. *Biochim. Biophys. Acta*. 1496:23–35.

Bement, W.M., H.A. Benink, and G. von Dassow. 2005. A microtubule-dependent zone of active RhoA during cleavage plane specification. *J. Cell Biol.* 170:91–101.

Bennett, V., and A.J. Baines. 2001. Spectrin and ankyrin-based pathways: metazoan inventions for integrating cells into tissues. *Physiol. Rev.* 81:1353–1392.

Bray, D., and J.G. White. 1988. Cortical flow in animal cells. *Science*. 239:883–888.

Bretscher, A. 1991. Microfilament structure and function in the cortical cytoskeleton. *Annu. Rev. Cell Biol.* 7:337–374.

Bretscher, A., K. Edwards, and R.G. Fehon. 2002. ERM proteins and merlin: integrators at the cell cortex. *Nat. Rev. Mol. Cell Biol.* 3:586–599.

Brieher, W.M., M. Coughlin, and T.J. Mitchison. 2004. Fascin-mediated propulsion of *Listeria monocytogenes* independent of frequent nucleation by the Arp2/3 complex. *J. Cell Biol.* 165:233–242.

Castellano, F., P. Chavrier, and E. Caron. 2001. Actin dynamics during phagocytosis. *Semin. Immunol.* 13:347–355.

Charras, G.T., and M.A. Horton. 2002. Single cell mechanotransduction and its modulation analyzed by atomic force microscope indentation. *Biophys. J.* 82:2970–2981.

Charras, G.T., J.C. Yarrow, M.A. Horton, L. Mahadevan, and T.J. Mitchison. 2005. Non-equilibration of hydrostatic pressure in blebbing cells. *Nature*. 435:365–369.

Cramer, L.P., M. Siebert, and T.J. Mitchison. 1997. Identification of novel graded polarity actin filament bundles in locomoting heart fibroblasts: implications for the generation of motile force. *J. Cell Biol.* 136:1287–1305.

Cunningham, C.C. 1995. Actin polymerization and intracellular solvent flow in cell surface blebbing. *J. Cell Biol.* 129:1589–1599.

Cunningham, C.C., J.B. Gorlin, D.J. Kwiatkowski, J.H. Hartwig, P.A. Janmey, H.R. Byers, and T.P. Stossel. 1992. Actin-binding protein requirement for cortical stability and efficient locomotion. *Science*. 255:325–327.

Cunningham, C.C., R. Vegners, R. Bucki, M. Funaki, N. Korde, J.H. Hartwig, T.P. Stossel, and P.A. Janmey. 2001. Cell permeant polyphosphoinositide-binding peptides that block cell motility and actin assembly. *J. Biol. Chem.* 276:43390–43399.

Dai, J., and M.P. Sheetz. 1999. Membrane tether formation from blebbing cells. *Biophys. J.* 77:3363–3370.

Defacque, H., M. Egeberg, A. Habermann, M. Diakonova, C. Roy, P. Mangeat, W. Voelter, G. Marriott, J. Pfannstiel, H. Faulstich, and G. Griffiths. 2000. Involvement of ezrin/moesin in de novo actin assembly on phagosomal membranes. *EMBO J.* 19:199–212.

Denker, S.P., and D.L. Barber. 2002. Cell migration requires both ion translocation and cytoskeletal anchoring by the Na-H exchanger NHE1. *J. Cell Biol.* 159:1087–1096.

Etienne-Manneville, S., and A. Hall. 2002. Rho GTPases in cell biology. *Nature*. 420:629–635.

Fishkind, D.J., L.G. Cao, and Y.L. Wang. 1991. Microinjection of the catalytic fragment of myosin light chain kinase into dividing cells: effects on mitosis and cytokinesis. *J. Cell Biol.* 114:967–975.

Fowler, V.M., N.J. Greenfield, and J. Moyer. 2003. Tropomodulin contains two actin filament pointed end-capping domains. *J. Biol. Chem.* 278:40000–40009.

Gautreau, A., D. Louvard, and M. Arpin. 2000. Morphogenic effects of ezrin require a phosphorylation-induced transition from oligomers to monomers at the plasma membrane. *J. Cell Biol.* 150:193–203.

Guha, M., M. Zhou, and Y.L. Wang. 2005. Cortical actin turnover during cytokinesis requires myosin II. *Curr. Biol.* 15:732–736.

Hamill, O.P., and B. Martinac. 2001. Molecular basis of mechanotransduction in living cells. *Physiol. Rev.* 81:685–740.

Higashida, C., T. Miyoshi, A. Fujita, F. Oceguera-Yanez, J. Monypenny, Y. Andou, S. Narumiya, and N. Watanabe. 2004. Actin polymerization-driven molecular movement of mDia1 in living cells. *Science*. 303:2007–2010.

Kamijo, K., N. Ohara, M. Abe, T. Uchimura, H. Hosoya, J.S. Lee, and T. Miki. 2006. Dissecting the role of Rho-mediated signaling in contractile ring formation. *Mol. Biol. Cell*. 17:43–55.

Lee, J.H., T. Katakai, T. Hara, H. Gonda, M. Sugai, and A. Shimizu. 2004. Roles of p-ERM and Rho-ROCK signaling in lymphocyte polarity and uropod formation. *J. Cell Biol.* 167:327–337.

Mangeat, P.H., and K. Burridge. 1984. Immunoprecipitation of nonerythrocyte spectrin within live cells following microinjection of specific antibodies: relation to cytoskeletal structures. *J. Cell Biol.* 98:1363–1377.

May, R.C., and L.M. Machesky. 2001. Phagocytosis and the actin cytoskeleton. *J. Cell Sci.* 114:1061–1077.

Mills, J.C., N.L. Stone, J. Erhardt, and R.N. Pittman. 1998. Apoptotic membrane blebbing is regulated by myosin light chain phosphorylation. *J. Cell Biol.* 140:627–636.

Rossman, K.L., C.J. Der, and J. Sondek. 2005. GEF means go: turning on RHO GTPases with guanine nucleotide-exchange factors. *Nat. Rev. Mol. Cell Biol.* 6:167–180.

Rybakin, V., and C.S. Clemen. 2005. Coronin proteins as multifunctional regulators of the cytoskeleton and membrane trafficking. *Bioessays*. 27:625–632.

Sakamoto, T., J. Limouze, C.A. Combs, A.F. Straight, and J.R. Sellers. 2005. Blebbistatin, a myosin II inhibitor, is photoinactivated by blue light. *Biochemistry*. 44:584–588.

Sanders, S.L., and C.M. Field. 1994. Cell division. Septins in common? *Curr. Biol.* 4:907–910.

Satterwhite, L.L., and T.D. Pollard. 1992. Cytokinesis. *Curr. Opin. Cell Biol.* 4:43–52.

Small, J.V., T. Stradal, E. Vignal, and K. Rottner. 2002. The lamellipodium: where motility begins. *Trends Cell Biol.* 12:112–120.

Spiliotis, E.T., M. Kinoshita, and W.J. Nelson. 2005. A mitotic septin scaffold required for Mammalian chromosome congression and segregation. *Science*. 307:1781–1785.

Spoerl, Z., M. Stumpf, A.A. Noegel, and A. Hasse. 2002. Oligomerization, F-actin interaction, and membrane association of the ubiquitous mammalian coronin 3 are mediated by its carboxyl terminus. *J. Biol. Chem.* 277:48858–48867.

Stossel, T.P., J. Condeelis, L. Cooley, J.H. Hartwig, A. Noegel, M. Schleicher, and S.S. Shapiro. 2001. Filamins as integrators of cell mechanics and signalling. *Nat. Rev. Mol. Cell Biol.* 2:138–145.

Straight, A.F., C.M. Field, and T.J. Mitchison. 2005. Anillin binds nonmuscle myosin II and regulates the contractile ring. *Mol. Biol. Cell*. 16:193–201.

Svitkina, T.M., and G.G. Borisy. 1998. Correlative light and electron microscopy of the cytoskeleton of cultured cells. *Methods Enzymol.* 298:570–592.

Totsukawa, G., Y. Yamakita, S. Yamashiro, D.J. Hartshorne, Y. Sasaki, and F. Matsumura. 2000. Distinct roles of ROCK (Rho-kinase) and MLCK in spatial regulation of MLC phosphorylation for assembly of stress fibers and focal adhesions in 3T3 fibroblasts. *J. Cell Biol.* 150:797–806.

Tran Quang, C., A. Gautreau, M. Arpin, and R. Treisman. 2000. Ezrin function is required for ROCK-mediated fibroblast transformation by the Net and Dbl oncogenes. *EMBO J.* 19:4565–4576.

Trinkaus, J.P. 1973. Surface activity and locomotion of Fundulus deep cells during blastula and gastrula stages. *Dev. Biol.* 30:69–103.

Vanni, C., A. Parodi, P. Mancini, V. Visco, C. Ottaviano, M.R. Torrisi, and A. Eva. 2004. Phosphorylation-independent membrane relocalization of ezrin following association with Dbl in vivo. *Oncogene*. 23:4098–4106.

Verkhovsky, A.B., T.M. Svitkina, and G.G. Borisy. 1995. Myosin II filament assemblies in the active lamella of fibroblasts: their morphogenesis and role in the formation of actin filament bundles. *J. Cell Biol.* 131:989–1002.

Wu, J.Q., J.R. Kuhn, D.R. Kovar, and T.D. Pollard. 2003. Spatial and temporal pathway for assembly and constriction of the contractile ring in fission yeast cytokinesis. *Dev. Cell*. 5:723–734.